DIGITAL DEMODULATION OF A FRACTIONAL FRINGE INTERFEROMETER

Christopher A. Belk and Tristan J. Tayag

Texas Christian University
Department of Engineering
TCU Box 298640
Fort Worth, Texas 76129

Abstract

Fractional fringe interferometers are capable of vibration displacement measurements that are many orders of magnitude less than the optical probe wavelength. But to achieve this high sensitivity, sophisticated demodulation techniques are required. We have constructed a fiber optic interferometer, which is based on pseudo-heterodyne modulation. We are using the TMS320 digital signal processor to implement a digital demodulation scheme to extract a target's vibration amplitude. The TMS320 first uses the Goertzel algorithm to detect a specific frequency within the spectrum of the interferometer's pseudo-heterodyne signal and then it manipulates this signal to compute the target's vibration amplitude. The theoretical background of the interferometer's demodulation scheme and preliminary experimental results from the digital demodulation will be presented.

1. INTRODUCTION

The calibration of transducers and instruments used in measuring motion quantities can be accomplished using interferometric techniques [Ref. 1]. Such small displacement measurements often require the application of a fractional fringe interferometer. Fractional fringe interferometry is a method of measuring target displacements less than the wavelength of the optical probe based on the interference pattern of two beams of light. Fractional fringe interferometers are capable of measuring displacements which are several orders of magnitude smaller than fringe counting methods. However, fractional fringe interferometers require that the target of interest exhibits sinusoidal displacement. Digital signal processing techniques can be utilized to demodulate the fractional fringe interferometer output signal to extract the displacement amplitude of the vibrating target.

In this paper, we present a scheme to digitally demodulate a fractional fringe interferometer. In section 2.1, we discuss the theory associated with fractional fringe interferometry. A scheme to demodulate the interferometer output signal using the Goertzel algorithm is then presented in section 2.2. Finally, preliminary experimental results concerning the interferometer and the Goertzel algorithm are given in section 3.

2. THEORY

2.1. Interferometry

An interferometer can be used to measure the displacement amplitude of a vibrating target based on the interference pattern formed by two beams of light. A fiber optic interferometer in the Michelson configuration is

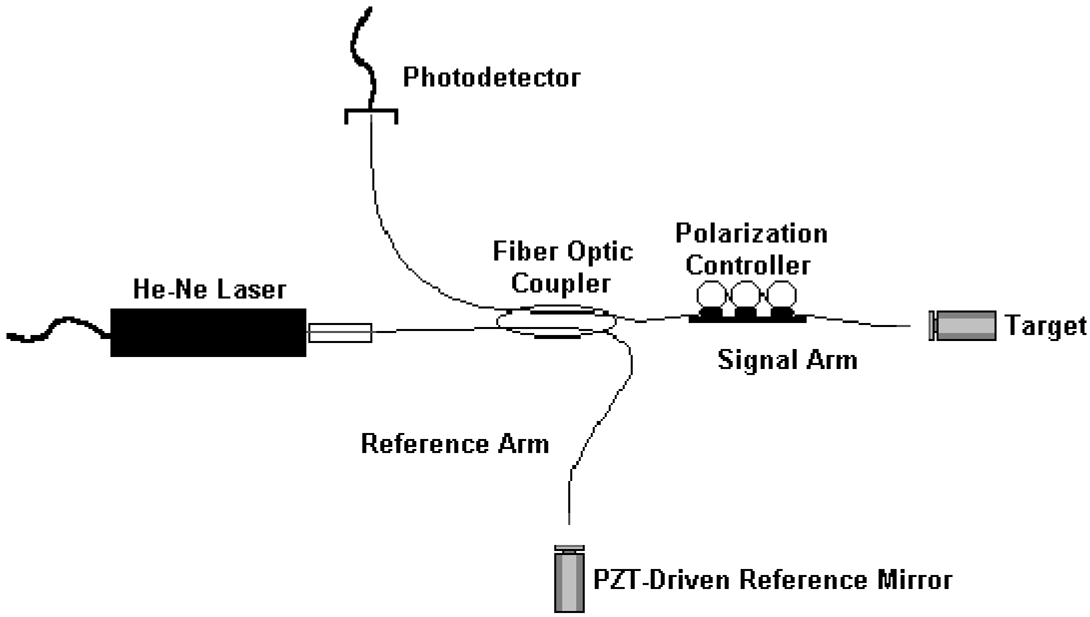

Figure 1. Fiber optic interferometer in the Michelson configuration.

shown in Figure 1. Six hundred, thirty-three nanometer wavelength light from a helium neon (HeNe) laser is split with a fiber optic coupler to form a signal arm and a reference arm. A piezoelectric transducer (PZT) driven mirror sinusoidally vibrating at a known amplitude and frequency reflects the reference beam back to the fiber optic coupler. The target vibrates with sinusoidal displacement at a known frequency and with an unknown amplitude. The signal beam is reflected from the target toward the fiber optic coupler. The fiber optic coupler combines the reference and signal beams to form an interference pattern. To maximize the fringe contrast of the interference pattern, a polarization controller [Ref. 2] is utilized in the signal leg to allow the polarization of the two beams to coincide. The photodetector then converts the power of the interference pattern into a current signal containing information regarding the displacement amplitude of the vibrating target.

The electric field of the reference beam is

$$E_r = \mathrm{Re}\{E_{r0} \exp[j(\omega_0 t - 2k_f x_{rf} - 2kx_{ra} + \phi_r)]\}, \tag{1}$$

where

E_{r0} = complex reference field amplitude,
ω_0 = optical angular frequency,
k_f = propagation constant in the single mode optical fiber,
x_{rf} = distance from the fiber optic coupler to the end of the reference arm fiber,
k = propagation constant in air,
x_{ra} = distance from the end of the fiber to the reference mirror, and
ϕ_r = phase shift introduced by the fiber optic coupler.

Similarly, the electric field of the signal beam is

$$E_s = \mathrm{Re}\{E_{s0} \exp[j(\omega_0 t - 2k_f x_{sf} - 2kx_{sa} + \phi_s)]\}, \tag{2}$$

where

E_{s0} = complex reference field amplitude,
x_{sf} = distance from the fiber optic coupler to the end of the signal arm fiber,
x_{sa} = distance from the end of the fiber to the target mirror, and
ϕ_s = phase shift introduced by the fiber optic coupler.

Assuming unity fringe contrast of the two interfering fields and ignoring terms that vary at optical frequencies, the photodetector's output current has the form [Ref. 2]

$$I_p \propto \mathrm{Re}\{E_{r0}E_{s0}^*\}\cos(\Phi' + 2k\delta), \tag{3}$$

where

δ= target displacement,
Φ' = static optical path length difference between the signal and reference arms, and
$\Phi' + 2k\delta \equiv -2k(x_{ra} - x_{sa}) - 2k_f(x_{rf} - x_{sf}) + \phi_r - \phi_s$.

Assuming that the target has a sinusoidal vibration at a known angular frequency ω_t, unknown amplitude a, and phase relative to the stimulus ϕ_t, the photodetector output current is

$$I_p \propto \mathrm{Re}\{E_{r0}E_{s0}^*\}\cos[\Phi' + 2ka\sin(\omega_t t + \phi_t)]. \tag{4}$$

We allow the reference mirror to vibrate about the static optical path length difference Φ' with a vibration amplitude of half a wavelength. Substituting $\Phi + \pi\sin(\omega_d t + \phi_d)$ for Φ' in equation (4) results in

$$I_p \propto \mathrm{Re}\{E_{r0}E_{s0}^*\}\cos[\Phi + \pi\sin(\omega_d t + \phi_d) + 2ka\sin(\omega_t t + \phi_t)], \tag{5}$$

where

Φ = optical path length difference bias point,
ω_d = reference mirror frequency, and
ϕ_d = phase relative to the stimulus.

Equation (5) may be expanded using the Fourier-Bessel relationships [Ref. 3] to yield

$$\begin{aligned} I_p \propto\ & \cos(\Phi)J_0(\pi)J_0(2ka) \\ & 2\sin(\Phi)J_0(\pi)J_1(2ka)\sin(\omega_t t + \phi_t) \\ & -2\sin(\Phi)J_1(\pi)J_0(2ka)\sin(\omega_d t + \phi_d) \\ & +2\cos(\Phi)J_0(\pi)J_2(2ka)\cos(2\omega_t t + 2\phi_t) \\ & +2\cos(\Phi)J_2(\pi)J_0(2ka)\cos(2\omega_d t + 2\phi_d) \\ & -2\sin(\Phi)J_0(\pi)J_3(2ka)\sin(3\omega_t t + 3\phi_t) \\ & -2\sin(\Phi)J_3(\pi)J_0(2ka)\sin(3\omega_d t + 3\phi_d) \ldots, \end{aligned} \tag{6}$$

where J_i is a Bessel function of the first kind of order i.

Assuming that the interferometer is stabilized at quadrature [Ref. 4], the optical path length bias point Φ will be $\pi/2$. Equation (6) then becomes

$$\begin{aligned} I_p \propto\ & -2J_0(\pi)J_1(2ka)\sin(\omega_t t + \phi_t) \\ & -2J_1(\pi)J_0(2ka)\sin(\omega_d t + \phi_d) \\ & -2J_0(\pi)J_3(2ka)\sin(3\omega_t t + 3\phi_t) \\ & -2J_3(\pi)J_0(2ka)\sin(3\omega_d t + 3\phi_d) \ldots. \end{aligned} \tag{7}$$

The vibrational amplitude *a* of the target is contained within the frequency components of the photodetector output signal. In the following section, we describe a demodulation scheme based on digital signal processing techniques to determine the target's vibrational amplitude.

2.2. Demodulation

The unknown amplitude of the target can be determined under the quadrature condition by mathematically manipulating one of the frequency components. With the interferometer stabilized at quadrature, the magnitude *S* of the dither frequency's third harmonic is

$$S \propto 2J_3(\pi)J_0(2ka). \tag{8}$$

Associated with the frequency component *S* is an unknown constant of proportionality *K*. The constant of proportionality K depends on both the photodetector gain and fringe contrast. To eliminate this constant of proportionality, a calibration factor must be determined when the target amplitude is zero. The calibration factor S_0 of the dither frequency's third harmonic is

$$S_0 = 2KJ_3(\pi). \tag{9}$$

Given this calibration factor, the constant of proportionality can then be eliminated by taking the ratio of equations (8) and (9)

$$S/S_0 = J_0(2ka). \tag{10}$$

The desired target amplitude *a* can then be determined from equation (10) by using a lookup table for a zero order Bessel function of the first kind. However, a technique to determine the magnitude of the frequency component *S* must first be implemented.

The magnitude of the frequency component of the photodetector current signal given in equation (8) can be determined using the digital signal processing techniques. We have chosen the Goertzel algorithm to extract the magnitude of the desired frequency component from the sampled photodetector current signal. A block diagram representation of the Goertzel algorithm as a two-pole digital resonator is shown in Figure 2. In this form, the Goertzel algorithm [Ref. 5] can be expressed by the difference equations

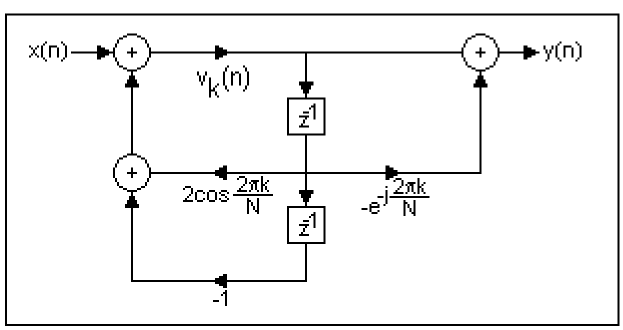

Figure 2. Direct Form II block diagram of the Goertzel algorithm.

Operations	Direct DFT	DIT FFT	DIF FFT	GA
Complex Multiplications*	8	7	7	0
Complex Additions*	7	7	3	0
Real Multiplications	0	0	0	11
Real Additions	0	0	4	19
Total Multiplications	32	28	28	11
Total Additions	30	28	24	19
TOTAL COMPUTATIONS	**62**	**56**	**52**	**30**

Table 1. Direct DFT, DIT FFT, DIF FFT, and Goertzel algorithm computational complexity comparison for calculating 1 frequency component of an 8-pt sequence.

*Note: One complex multiplication = 4 real multiplications and 2 real additions.
One complex addition = 2 real additions.

$$v_k(n) = 2\cos(2\pi k/N)v_k(n-1) - v_k(n-2) + x(n), \text{ and} \tag{11}$$

$$y_k(n) = v_k(n) - W_N^k v_k(n-1), \tag{12}$$

where

k = the DFT frequency bin number,
n = sample number,
N = sample record length,
$v_k(-1) = 0$,
$v_k(-2) = 0$,
$x(n)$ = input signal,
$y(n)$ = output signal,
$j = \sqrt{-1}$, and
$W_N = \exp(-j2\pi/N)$.

To compute a frequency point of the DFT, the recursive equation (11) is executed for $n = 0, 1, \ldots, N$, whereas equation (12) is calculated only when $n = N$. The result of the two-pole resonator form of the Goertzel algorithm is two symmetrical points of the DFT. The computational complexity of the Goertzel algorithm requires $N + 3$ real multiplications and $2N + 3$ real additions. When a relatively few number of frequency components are to be determined, the Goertzel algorithm is a computationally more efficient method than the fast Fourier transform (FFT) for calculating the DFT. A comparison of the computational efficiency of the direct DFT, the decimation-in-time (DIT) FFT, the decimation-in-frequency (DIF) FFT, and the Goertzel algorithm (GA) for determining one frequency component of an 8-point sequence is given in Table 1. Given the efficiency of the Goertzel algorithm, it was chosen for use in our demodulation scheme.

3. EXPERIMENT

The interferometer setup considered in our research is similar to the configuration shown in Figure 1. By applying a 100 Hz sinusoidal vibration to the reference arm and a 1 kHz sinusoidal vibration to the signal arm, we obtained the frequency spectrum of the photodetector output as shown in Figure 3. The magnitudes of the frequency components contain information regarding the vibrational amplitude of the target.

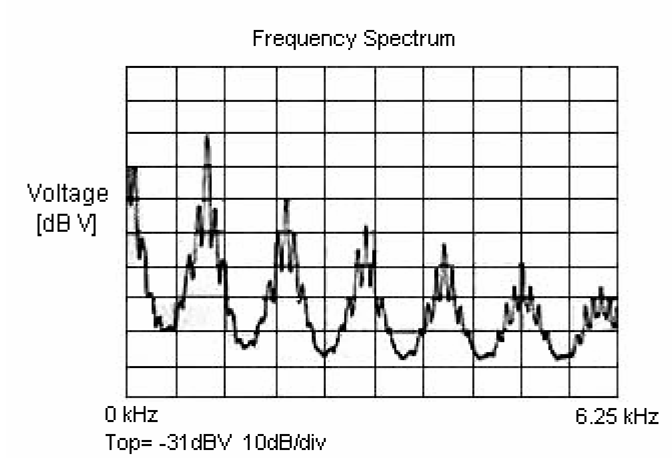

Figure 3. Photodetector output current frequency spectrum.

To detect a specific frequency component of the photodetector output current, an assembly language program that executes the Goertzel algorithm was written for the Texas Instruments (TI) TMS320C31 Digital Signal Processing Starter's Kit (DSK). The following parameters were chosen for program development:

Sampling rate = 20 kHz,
Detected frequency = 658 Hz,
Analog-to-digital converter voltage range = ±1.5 V, and
Sample record length N = 3000.

Operation of the Goertzel program was verified by applying well-defined input signals to the DSK as shown in Figure 4. The program was characterized for frequency selectivity and accuracy. To test the frequency selectivity of the Goertzel program, we considered the Fourier series expansion of a periodic square wave as shown in Figure 5. A 1 V_{pk} periodic square wave with a fundamental frequency of 658 Hz was used as the input to the Goertzel program. The Goertzel program selected only the frequency component corresponding to 658 Hz and returned a DC output approximately equal to $4/\pi$ times the square wave amplitude as shown in Figure 6a. The fundamental frequency of the square wave input was then changed to 219 Hz. Figure 6b shows that the DC output of the Goertzel algorithm corresponds to the correct magnitude of the square wave's third harmonic. Finally, to observe how well the Goertzel program rejected other frequency bins of the DFT, the frequency of the input square wave was set to 665 Hz. In Figure 6c note that the DC output of the Goertzel program was zero.

The accuracy of the Goertzel algorithm was tested using a 658 Hz input sinusoid. A three-sample window

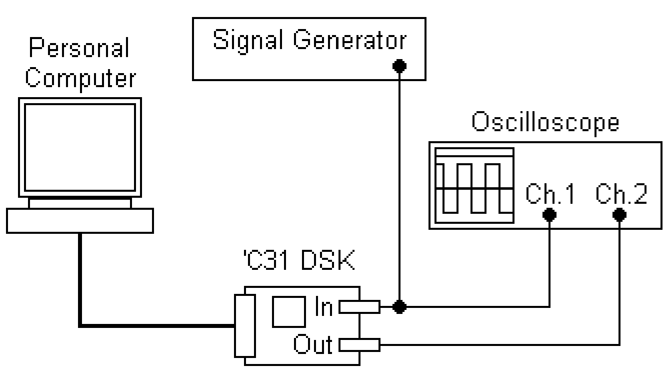

Figure 4. Goertzel program test setup.

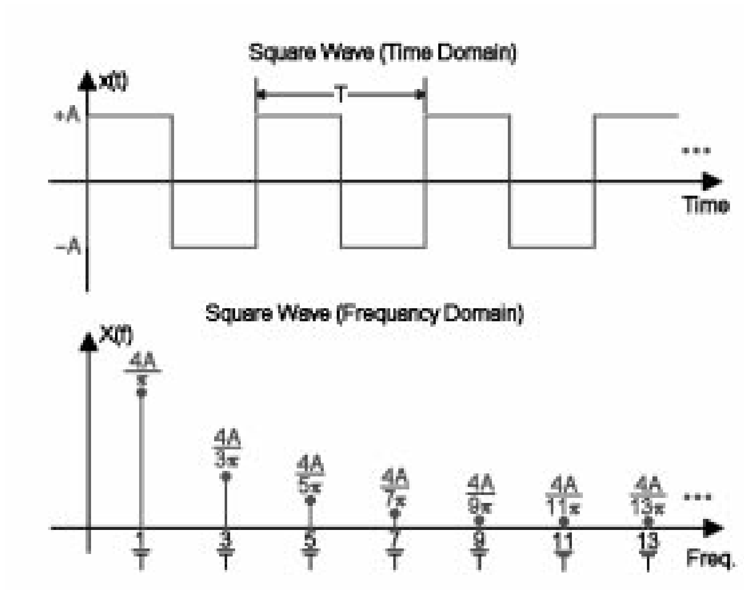

Figure 5. Square wave Fourier series expansion.

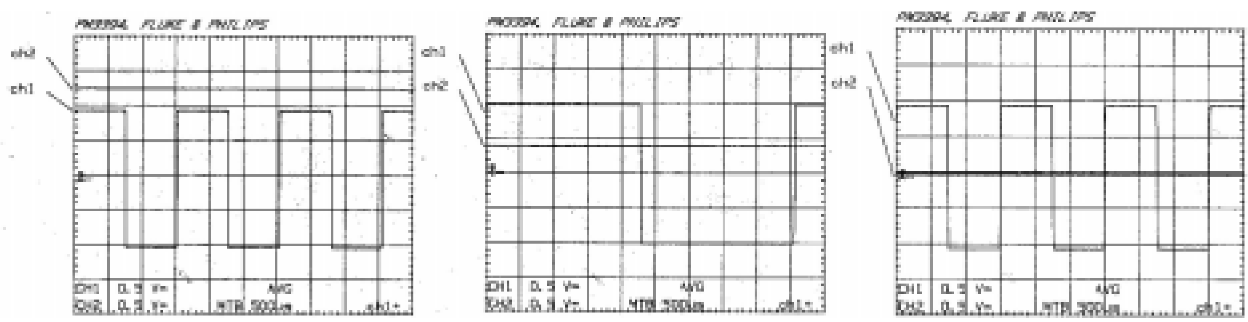

a) Input Ch.1: 1 V_{pk} 658 Hz
Output Ch.2: 1.25 V DC

b) Input Ch.1: 1 V_{pk} 219 Hz
Output Ch.2: 0.4 V DC

c) Input Ch.1: 1 V_{pk} 665 Hz
Output Ch.2: 0 V DC

Figure 6. Goertzel algorithm frequency selectivity test results.

peak detection program was used to determine the TMS320 floating-point representation of the sinusoidal peak value to compare with the floating-point output value of the Goertzel program. The amplitude of the input signal was varied over the allowable range of the analog-to-digital converter. Figure 7 shows an approximate 5-6% error between the peak detection and Goertzel programs for peak-to-peak input voltages greater than 0.5 $V_{pk\text{-}pk}$. It is believed that the error was due to quantization noise in the Goertzel program. Applying a correction factor at the output of the Goertzel program will be used to correct for this error.

4. SUMMARY AND CONCLUSIONS

In this paper, we presented a novel demodulation scheme for a fractional fringe interferometer. This scheme uses digital signal processing techniques to determine the subwavelength displacement amplitude of a sinusoidally vibrating target. First, the theoretical principles and mathematical concepts concerning fractional fringe interferometry were explained. Following the explanation was a discussion concerning the Goertzel algorithm, a

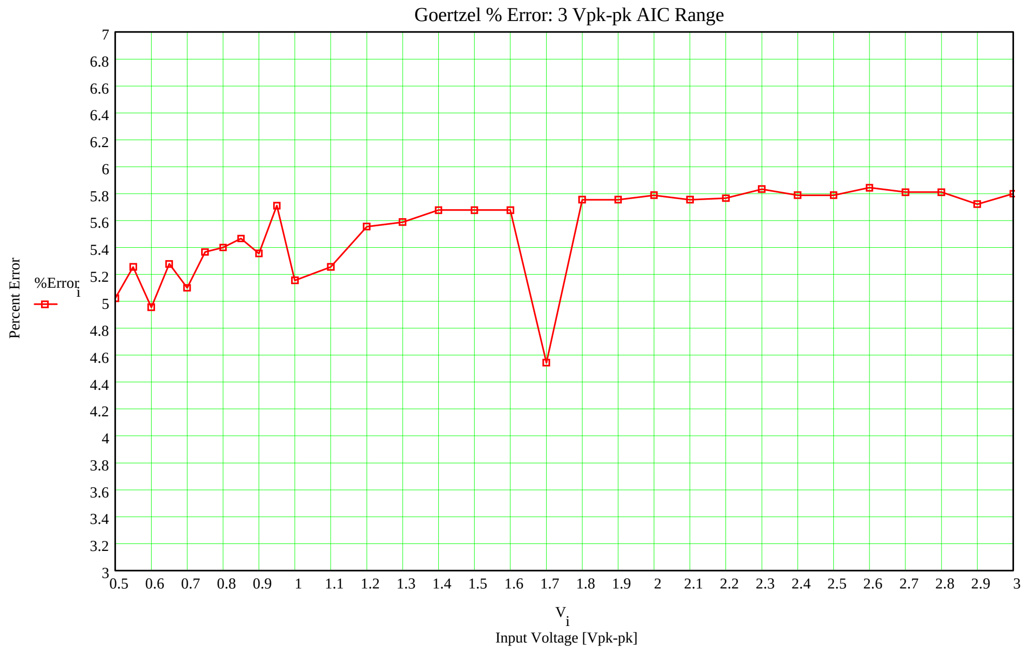

Figure 7. Goertzel program accuracy test results.

discrete Fourier transform calculation method, and its use in the demodulation scheme. Preliminary experimental results concerning the Goertzel algorithm as programmed on the Texas Instruments TMS320C31 DSK were also given. Specifically, the frequency selectivity and accuracy of the Goertzel algorithm were characterized.

5. REFERENCES

[1] Link, A., and von Martens, H.-J., "Amplitude and Phase Measurement of Sinusoidal Vibration in the Nanometer Range Using Laser Interferometry", Measurement, vol. 24, pp. 55-67 (1998).

[2] Lefever, H.C., "Single-Mode Fibre Fractional Wave Devices and Polarization Controllers", Electron. Lett., vol. 16, p. 778 (1980).

[3] Kreyzig, E. Advanced Engineering Mathematics, 4th ed., John Wiley & Sons, Inc., New York (1979).

[4] Haraharan, P., Optical Interferometry, Academic Press, Orlando (1985).

[5] Proakis, J. G., and Manolakis, D. G., Digital Signal Processing Principles, Algorithms, and Applications, Prentice Hall, New Jersey, pp. 480-481 (1996).